Coordination Chemistry Reviews
208 (2000) 213–225

COORDINATION CHEMISTRY REVIEWS

www.elsevier.com/locate/ccr

Synthesis, spectroscopic and a ZINDO study of *cis*- and *trans*-(X_2)bis(4,4′-dicarboxylic acid-2,2′-bipyridine)ruthenium(II) complexes ($X = Cl^-$, H_2O, NCS^-)

Md. K. Nazeeruddin [a],*, S.M. Zakeeruddin [a],
R. Humphry-Baker [a], S.I. Gorelsky [b], A.B.P. Lever [b],
M. Grätzel [a]

[a] *Laboratory for Photonics and Interfaces, Institute of Physical Chemistry, Swiss Federal Institute of Technology, CH-1015 Lausanne, Switzerland*
[b] *Department of Chemistry, York University, Toronto, Ont., Canada M3J 1P3*

Received 14 October 1999; received in revised form 21 December 1999; accepted 21 December 1999

Contents

---

* Corresponding author. Fax: + 41-21-6934111.
E-mail address: mdkhaja.nazeeruddin@epfl.ch (Md.K. Nazeeruddin).

PII: S0010-8545(00)00338-6

Abstract

Ruthenium complexes of the type *trans*-[Ru(dcbpyH_2)$_2$(Cl)$_2$], *trans*-[Ru(dcbpyH_2)$_2$(H_2O)$_2$] and *trans*-[Ru(dcbpyH_2)$_2$(NCS)$_2$] (dcbpyH_2 = 4,4′-dicarboxylic acid-2,2′-bipyridine) were synthesized and characterized by NMR, UV–vis absorption and emission spectroscopy. The proton NMR spectra of the *trans* isomers, in the aromatic region, show only three peaks corresponding to the two dcbpy ligands in which all the pyridine rings are *trans* to each other and magnetically equivalent. The ^{13}C-NMR spectrum of the *trans* isomer is characterized by a relatively simple pattern of resonances from the four equivalent pyridine rings. The lowest energy metal-to-ligand charge-transfer transition maximum of the *trans*-[Ru(dcbpyH_2)$_2$(Cl)$_2$] complex is at 14500 cm^{-1} in DMF solution and shows onset of weak and broad emission signals above 11100 cm^{-1}. This is a significantly larger red shift compared with any of the *trans* ruthenium(II) polypyridyl complexes reported to date. The absorption and emission maxima of the *trans* complexes are red shifted compared with the *cis* analogues, which is due to the CO_2H contribution in the *trans* isomer that stabilizes the LUMO relative to the LUMO of the *cis* isomer. The enhanced red response of the *trans* complexes renders them as suitable dyes for dye-sensitized titanium dioxide mesoporous electrodes. The electronic spectra of *cis*- and *trans*-[Ru(dcbpyH_2)$_2$(Cl)$_2$] complexes were calculated by ZINDO/S and compared with the experimental data.

Keywords: Spectroscopic; ZINDO study; Ruthenium complexes; *cis*-*trans* Isomers; Sensitizers

---

1. Introduction

Ruthenium polypyridyl complexes have been studied extensively for many years [1,2] in part because of their possible applications in energy conversion processes [3,4]. The majority of the ruthenium complexes reported, containing two bipyridyl and two monodentate ligands, have a *cis* configuration [2b], although the synthesis and crystal structure of a few *trans* complexes have been described [5,6]. A case of particular interest is the *cis*-[Ru(dcbpyH_2)$_2$(NCS)$_2$] complex. This complex is one of the most efficient heterogeneous charge transfer sensitizers known to date and is widely used in the nanocrystalline TiO_2 solar cell [4,7–12]. The present paper reports the synthesis and characterization of *trans* isomers of [Ru(dcbpyH_2)$_2$(X)$_2$] (where X = Cl^-, H_2O, NCS^-).

2. Experimental

2.1. Analytical measurements

UV–vis and fluorescence spectra were recorded in a 1-cm path length quartz cell on a Cary 5 spectrophotometer and a Spex Fluorolog 112 Spectrofluorometer, respectively. The emitted light was detected with a Hamamatsu R2658 photomultiplier operated in single photon counting mode. The emission spectra were photometrically corrected using a calibrated 200W tungsten lamp as a reference source.

A dilute solution of quinine sulfate was used as quantum yield standard. The solutions were prepared to give approximate concentrations of 10 μM, and purged with nitrogen. The emission lifetimes were measured by exciting the sample with a pulse from an active modelocked Nd YAG laser using the frequency doubled line at 532 nm. The emission decay was followed on a Tektronix TDS 640 A Digitizing Oscilloscope using a Hamamatsu R928 photomultiplier to convert the light signal to a voltage waveform. Proton and ^{13}C-NMR spectra were measured on a Bruker 200 MHz spectrometer and the reported chemical shifts were against TMS.

2.2. Synthesis

The *cis*-[Ru(dcbpyH$_2$)$_2$(Cl)$_2$], *cis*-[Ru(dcbpyH$_2$)$_2$(H$_2$O)$_2$] and *cis*-[Ru(dcbpyH$_2$)$_2$(NCS)$_2$] were synthesized using the previously described procedure [4,13]. For convenience, hereafter, these complexes are referred to as *cis*-dichloro, *cis*-diaqua and *cis*-dithiocyanate complexes, respectively. Scheme 1 shows the details of the strategy adopted for the synthesis of the *trans* complexes. The chloride ligands in the *cis*-dichloro complex are labile to substitution and in coordinating solvents like water and DMSO, the chloride ligands are readily displaced to form the respective diaqua and dmso complexes. The *cis*-dichloro complex also undergoes photoinduced *cis*-to-*trans* isomerisation in organic solvents. Photolysis of the *cis*-dichloro complex in ethanol solution at room temperature (r.t.) resulted in the *trans*-dichloro complex as an insoluble product. Similarly, the *cis*-diaqua complex was dissolved in water at pH 3.5 and left under room light for several days to obtain the *trans*-diaqua complex as an insoluble product. The *trans*-dithiocyanato complex was synthesized by reacting the *trans*-dichloro complex in DMF solvent with an excess of ammonium thiocyanate under argon. The yield of the *trans*-dithiocyanate complex was low ($\approx$ 15%) even in the dark and at low temperature. The majority of the product that formed during the synthesis was the *cis*-dithiocyanato complex.

3. Results and discussion

3.1. NMR spectroscopic studies

The NMR data of these complexes are shown in Table 1. The NMR spectra of transition metal complexes are extremely useful to identify the *cis* and *trans* isomers. Because of the symmetry of the *cis*-isomers of the type [Ru(dcbpyH$_2$)$_2$(X)$_2$] (where $X = Cl^-$, H$_2$O, NCS$^-$) show six peaks in the aromatic region corresponding to two different pyridine ring protons in which two are *trans* to each other and the remaining two are *trans* to the X ligands (Table 1). The downfield shifted proton resonance peaks due to H-6, H-3 and H-5 were assigned to pyridine rings *trans* to each other, and the high field proton resonances to pyridine rings *trans* to X ligands [14]. On the other hand, the proton NMR spectra of the *trans* isomers in the aromatic region show only three peaks corresponding to the two dcbpy ligands in

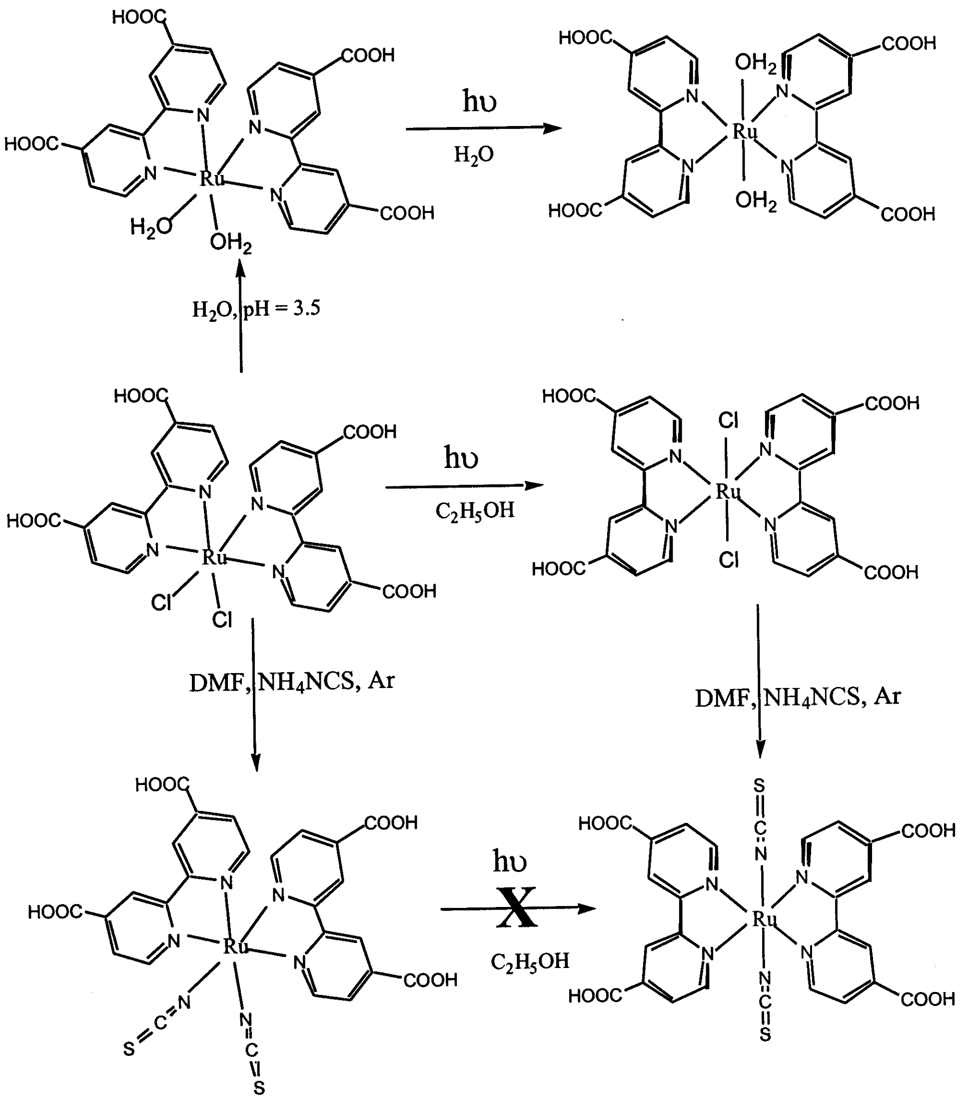

Scheme 1.

which all the pyridine rings are *trans* to each other and magnetically equivalent. It is interesting to note that the H-6 and H-5 proton peak positions in the *trans* configuration are very close to the corresponding peak positions in the *cis* configuration that were assigned to the pyridine *trans* to pyridine. However, there is a ≈ 0.1 ppm upfield shift of the H-6 proton compared with the *cis* isomer H-6 proton. The *trans*-dichloro complex shows 0.88 ppm chelation induced shifts (CIS, compared with the free ligand) for the H-6 proton because of dπ donation from the ligand to the metal centre. Nevertheless, the H-3 and H-5 protons show 0.47 and 0.36 ppm CIS values, respectively.

Table 1
^{1}H-NMR data of the aromatic region for ruthenium complexes and the ligand 4,4′-COOH-2,2-bipyridine in D_2O solution containing 0.05 M NaOD[a]

Complex/ligand	6	6′	5	5′	3	3′
dcbpy	8.78 (d)		7.87 (dd)		8.40 (d)	
cis-[Ru(dcbpyH$_2$)$_2$(Cl)$_2$][b]	9.84 (d)	7.80 (d)	8.13 (dd)	7.39 (dd)	8.86 (d)	8.69 (d)
cis-[Ru(dcbpyH$_2$)$_2$(NCS)$_2$]	9.55 (d)	7.82 (d)	8.22 (dd)	7.52 (dd)	8.94 (d)	8.77 (d)
cis-[Ru(dcbpyH$_2$)$_2$(H$_2$O)$_2$]	9.38 (d)	7.78 (d)	8.18 (dd)	7.50 (dd)	8.90 (d)	8.74 (d)
trans-[Ru(dcbpyH$_2$)$_2$(Cl)$_2$]	9.66 (d)	–	8.12 (dd)	–	8.87 (s)	–
trans-[Ru(dcbpyH$_2$)$_2$ (NCS)$_2$]	9.48 (d)	–	8.03 (d)	–	8.83 (s)	–
trans-[Ru(dcbpy)$_2$(H$_2$O)$_2$]	9.35 (b)	–	7.75 (b)	–	8.70 (b)	–

[a] In ppm with respect to TMS; (d), doublet; (dd), doublet of doublet; (s), singlet; (b), broad signal.

[b] After a few minutes of the solution preparation new resonances appear more upfield than those of the dichloro species due to substitution of the chloro ligands.

The proton decoupled ^{13}C-NMR spectra of the *cis* and *trans* isomers show different carbon resonances that were identified by comparison with known bipyridine complexes [15]. The ^{13}C-NMR spectra of *cis* isomers show 12 resonance peaks consisting of six sets due to two different dcbpy ligands. In the *cis*-dithiocyanato complex, besides these 12 peaks, there is a single resonance peak at 132.84 ppm, which is assigned to the carbon of the N-coordinated NCS. The ^{13}C-NMR spectrum of the *trans*-dithiocyanato isomer is characterized by a relatively simple pattern of resonances from the four equivalent pyridine rings. The pattern consists of six single resonance peaks coming from the dcbpy carbons and one resonance peak at 155.27 ppm, which was assigned to the *trans* NCS ligands. There is a noteworthy difference between the *cis*-NCS carbon resonance (132.84 ppm) and the *trans*-NCS resonance (155.27 ppm), which we attribute to deshielding of *trans*-NCS carbons. Since chemical shift is a measure of electron density around that atom, this indicates that in a *trans* configuration the thiocyanato ligands have less electron density due to the weak π back bonding from the ruthenium centre to the axial thiocyanate ligands compared with *cis*-NCS. Our finding for *trans*-NCS carbon resonance is consistent with a known ruthenium complex that contains *trans*-NCS ligands [16].

3.2. Electronic spectra

The *cis* and *trans* isomers in solution show a distinct difference in colour. The electronic properties of these isomers are considerably different and they are shown in Table 2. The UV–vis absorption spectrum of the *trans*-dichloro complex in DMF solution shows at least three metal-to-ligand charge-transfer (MLCT) absorption bands in the visible region at 14 500, 16 900 and 22 700 cm^{-1} (Fig. 1). The band in the UV at 31 200 cm^{-1} with a shoulder at 32 900 cm^{-1} is assigned to an intra ligand (π–π*) charge transfer transition [17]. On the other hand, the *cis*-

Table 2
Electronic spectral data of the *cis*- and *trans*-bis(4,4′-dicarboxylic acid-2,2′-bipyridine)ruthenium (X_2) complexes ($X = Cl^-$, H_2O, NCS^-) in DMF[a]

Complex	Absorption maximum (cm^{-1})[b] (ε 10^4 M^{-1} cm^{-1})			Emission $h_{\max}$ (cm^{-1}) at 298 K	τ (ns) at 298 K
cis-[Ru($dcbpyH_2$)$_2$(Cl)$_2$]	16 900 (1.1)	23 000 (1.0)	31 600 (3.45)	11 800	–
cis-[Ru($dcbpyH_2$)$_2$(H_2O)$_2$][c]	20 000 (1.19)	27 000 (1.09)	32 700 (4.92)	13 300[d]	–
cis-[Ru($dcbpyH_2$)$_2$(NCS)$_2$]	18 600 (1.42)	25 100 (1.40)	31 800 (4.82)	12 000	24
trans-[Ru($dcbpyH_2$)$_2$(Cl)$_2$]	14 500 (0.60), 16 900 (0.84)	22 700 (0.80),	31 300 (2.78)	> 11 100	–
trans-[Ru(dcbpy)$_2$(H_2O)$_2$]	18 900 (0.88)	26 300 (0.74)	32 100 (2.2)	12 500[d]	–
trans-[Ru($dcbpyH_2$)$_2$(NCS)$_2$]	17 200 (1.25), 18 900 (1.172)	24 900 (1.02)	31 800 (3.93)	11 500	12
cis-[Ru(bpy)$_2$(H_2O)$_2$][e]	20 800	–	–	15 200	–
trans-[Ru(bpy)$_2$(H_2O)$_2$][e]	20 200	–	–	14 300	–

[a] The emission spectra were obtained by exciting at the λ maximum of the complexes.

[b] The values in parentheses are ± 5%.

[c] Measured in water at pH 4.5.

[d] Weak and broad emission maximum.

[e] Reference [5b].

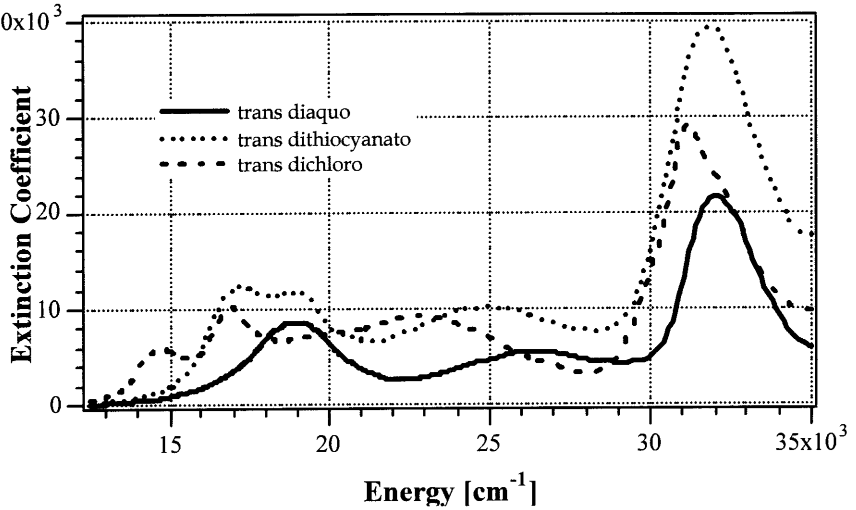

Fig. 1. UV–vis absorption spectra of *trans*-bis(2,2′-bipyridine-4,4′-dicarboxylic acid)ruthenium(II) (X_2) complexes ($X = Cl^-$, H_2O and NCS^-). The concentration of the solutions was 1.5×10^{-5} M in DMF, 1-cm cell. The *trans*-diaqua complex was measured in water.

dichloro complex in DMF solution shows only two distinct broad bands in the visible region at 16 900 and 23 000 cm^{-1}, which were assigned to a MLCT transition. The lowest energy MLCT band in the *trans*-dichloro complex (14500 cm^{-1}) was significantly red shifted compared with the *cis*-dichloro complex (16 900 cm^{-1}) and for any of the *trans*-Ru(II) polypyridyl complexes reported to date in the literature [5,6]. This red shift is due to stabilization of the LUMO of the dcbpyH_2 ligand in the *trans* species relative to the *cis*, as demonstrated below using ZINDO calculations (Section 4.3).

The *cis*-diaqua complex is insoluble in organic solvents such as ethanol, methanol, acetonitrile and acetone but soluble in water. The replacement of anionic chloride ligands by neutral aqua ligands blue shifts the lowest energy MLCT absorption maxima from 16 900 (measured in DMF) to 20 000 cm^{-1} (measured in H_2O). The observed blue shift of the *cis*-diaqua complex result from stabilization of the metal t_{2g} orbitals, which is in agreement with Lever's electrochemical parametrization of ligands for metal complexes [18]. The *trans*-diaqua complex in water shows two bands at 18 900 and 26 300 cm^{-1}. Nonetheless, the band at 18 900 cm^{-1} is broad and appears as a convolution of two bands.

The UV–vis absorption of the *trans*-dithiocyanato complex in DMF shows three intense MLCT bands at 24 900, 18 900 and 17 200 cm^{-1} (Table 2). The band at 31 800 cm^{-1} was assigned to the intra ligand π–π* transition of dcbpy ligand. The lowest energy MLCT maximum shifts from 18 600 to 17 200 cm^{-1} upon *cis*-to-*trans* isomerization. The interesting phenomenon of *trans* complexes is the presence of three broad visible bands compared with *cis* that has only two visible absorption bands.

The absorption maxima of *cis*- and *trans*-Ru(II)(2,2′-bipyridine)$_2$(H$_2$O)$_2$] has been reported at 20 800 and 20 300 cm^{-1}, respectively [5b]. Our data are consistent with the trend that the *trans* complexes are red shifted compared with the *cis* analogues [19].

The red shift (2700 cm^{-1}) of the lowest energy MLCT absorption in the spectrum of the *trans*-dichloro complex compared with the spectrum of the *trans*-dithiocyanato is due to the strong σ donar property of the Cl$^-$ compared with the NCS$^-$ ligand. The chloride ligands causes destabilization of the metal t$_{2g}$ orbitals, and raising them in energy closer to the ligand π* orbital results in lower energy MLCT transitions (Fig. 1). According to Lever's electrochemical parametrization the chloride ligand has a parameter value of -0.24 and the thiocyanate ligand has a value of -0.06. Our electrochemical and absorption data are in good agreement with reported parametrization scale for ligands [18].

The *trans* dichloro and dithiocyanate complexes are stable in ethanol at r.t. However, the *trans*-diaqua complex in aqueous solution slowly converts to the more stable *cis*-diaqua complex at r.t. Hesek et al. has observed, even under dark conditions, the formation of the more stable *cis*-Ru(II)(2,2′-bipyridine)$_2$(DMSO)$_2$] from *trans*-Ru(II)(2,2′-bipyridine)$_2$(H$_2$O)$_2$] in the presence of dmso solvent [6].

3.3. Emission spectra

The *trans*-dichloro complex in DMF solution at r.t. shows no detectable emission up to 11 100 cm^{-1}. However, the onset of a weak and broad emission signal is discernible above 11 100 cm^{-1}. Hence, the emission from the *trans*-chloro complex is expected to be in the 11 100–9100 cm^{-1} region, beyond the detector response of our equipment. Excitation of the *trans*-diaqua complex at 19 200 cm^{-1} in aqueous solution at r.t. shows a broad emission maxima centered at 12 500 cm^{-1}.

When excited in the lowest energy MLCT absorption band, the *trans*-dithiocyanato isomer in DMF solution at 298 K exhibits a luminescence consisting of a single band with a maximum at 11 500 cm^{-1} (Fig. 2). Excitation of these complexes at different wavelengths within the manifold of the MLCT bands gave the same emission maxima. This phenomenon shows that exciting the complex between 26 300 and 15 400 cm^{-1} leads to population of the same luminescent state. The excited state lifetimes of the *trans*- and *cis*-dithiocyanato isomer, measured at 298 K under aerobic conditions, are 12 and 24 (± 5) ns, respectively.

4. DFT and ZINDO calculations

4.1. Computational details

DFT calculations were carried out using Gaussian 98 [20] running on an SGI Origin 2000 computer, while ZINDO calculations used HyperChem 5.1 (Hypercube, Florida) [21] run on a PC Pentium II 400 MHz. Becke's three parameter hybrid functional [22] with LYP correlation functional [23] (B3LYP) and an effective core potential basis set LanL2DZ [24] was employed in the DFT calculations.

As a starting geometry for DFT calculations, we used an optimized geometry at the molecular-mechanics level. The electronic spectra of [Ru(dcbpyH_2)$_2$$Cl_2$] were calculated with ZINDO/S [21], utilizing the Ru parameters obtained from Ref. [25] and Cl parameters from Ref. [26]. The overlap weighting factors $\sigma-\sigma$ and $\pi-\pi$ were set at 1.265 and 0.585, respectively [21]. The number of singly excited configurations used was 1250 (e.g. 25 × 25 occupied x virtual orbitals).

4.2. Geometry optimization

The geometries of the *cis*- and *trans*-[Ru(dcbpyH_2)$_2$$Cl_2$] complexes were optimized with the B3LYP functional and using the LanL2DZ basis set. The structures of the complexes were optimized with no symmetry restraints. Geometry optimization of the *trans* isomer produced a structure with D_2 point group symmetry, while the *cis* isomer has C_2 point group symmetry. Both *cis*- and *trans*-[Ru(dcbpyH_2)$_2$$Cl_2$] complexes display a pseudooctahedral arrangement of ligands around the metal atom with a Cl–Ru–Cl angle of 180° for the *trans* and 93.2° for the *cis* isomer. The configuration of the dcbpyH_2 ligand compares favourably with those reported for other 2,2′-bipyridyl complexes [5b]. The average ring C–C and C–N bond lengths are 1.40 and 1.37 Å. The C–C bond length between the two aromatic rings of dcbpyH_2 ligand is 1.47 Å and is similar to the values reported in the bpy complexes. All carboxyl groups are in the same plane as the aromatic rings of the ligand. The calculated Ru–N distances (2.078 Å) in the *trans*-[Ru(dcbpyH_2)$_2$$Cl_2$] complex are close to those of a related complex, *trans*-[Ru(bpy)$_2$(OH_2)$_2$], where the Ru–N distances are 2.090(3) and 2.099(3) Å. The dihedral angle between the plane defined by Ru and two nitrogen atoms of one dcbpyH_2 ligand and that defined by Ru and the symmetry-related nitrogen atoms of the other dcbpyH_2 ligand was calculated to

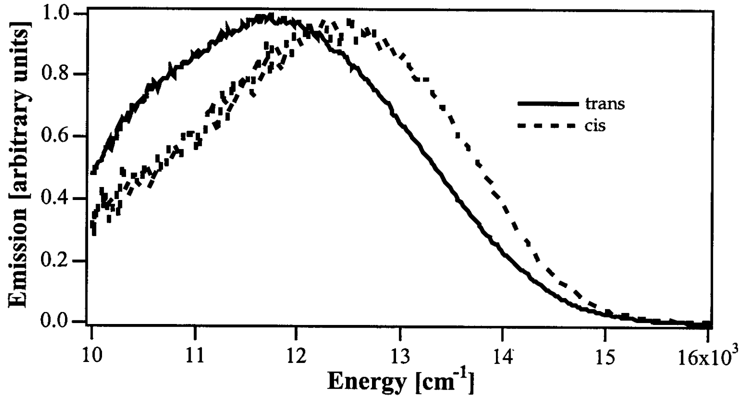

Fig. 2. Emission spectra of *cis* and *trans*-dithiocyanatobis(2,2′-bipyridine-4,4′-dicarboxylic acid)-ruthenium(II) complexes measured at 298 K under aerobic conditions in DMF solution.

be 22.5°. The Ru–N distances in the *cis* isomer (2.043 and 2.057 Å) also agree very well with those reported for *cis*-[Ru(dcbpyH$_2$)$_2$(NCS)$_2$], where the Ru–N distances are between 2.036(15) and 2.058(12) Å [14b].

4.3. Electronic spectra

The three highest occupied molecular orbitals (HOMO) for *cis*- and *trans*-[Ru(dcbpyH$_2$)$_2$(Cl)$_2$] complexes are mostly formed from 4d(Ru) orbitals. Their contribution ranges from 65 to 92% for the *trans* isomer, and from 70 to 80% for the *cis* isomer (Table 3). Other contributions to HOMO-2, 1, 0 come mainly from the 'dcbpyH$_2$' π orbitals. The lowest virtual orbitals are almost entirely localized on two dcbpyH$_2$ ligands with a contribution of 4d(Ru) orbitals (1–14% for *trans*, and 3–12% for the *cis* isomer). It is noteworthy that the dπ (b$_3$) Ru orbital directed towards the dcbpyH$_2$ ligands in the *trans* isomer is coupled to the π* orbitals of both dcbpyH$_2$ ligands and is thereby delocalized to a considerable degree, much

Table 3
Frontier molecular orbitals (ZINDO/S) of Ru(dcbpyH$_2$)$_2$Cl$_2$[a]

Orbital	*Γ* [b]	*ε* (eV)[c]	Atomic orbital contributions (%) from[d]		
			Ru	Cl	CO$_2$H
cis-Ru(dcbpyH$_2$)$_2$Cl$_2$ (C_2 point group)					
LUMO+3	b	−1.73	3.0	0.2	25.6
LUMO+2	a	−1.73	2.5	0.0	28.9
LUMO+1	a	−2.08	12.4	0.8	14.7
LUMO	b	−2.32	4.5	0.5	16.5
HOMO	a	−7.56	70.2	5.9	0.2
HOMO-1	b	−7.66	76.5	3.7	0.6
HOMO-2	a	−7.71	80.0	4.2	0.6
HOMO-3	b	−9.48	0.1	0.8	0.1
HOMO-4	a	−9.52	0.9	4.9	0.1
trans-Ru(dcbpyH$_2$)$_2$Cl$_2$ (D_2 point group)					
LUMO+3	b$_2$	−1.55	2.8	0.0	31.8
LUMO+2	b$_3$	−1.69	13.5	0.1	17.6
LUMO+1	a	−1.69	0.8	0.0	29.3
LUMO	b$_1$	−2.30	0.5	1.1	14.2
HOMO	b$_3$	−7.46	65.4	3.4	2.1
HOMO-1	b$_2$	−7.50	80.8	4.3	0.8
HOMO-2	a	−7.77	92.0	0.1	0.2
HOMO-3	b$_2$	−9.33	1.2	0.0	0.0
HOMO-4	a	−9.38	1.3	0.0	0.0

[a] HOMO, 101; LUMO, 102.

[b] Irreducible representation. For the *trans* isomer: *z* axis is Cl–Ru–Cl, *x* axis goes in between dcbpyH$_2$ ligands.

[c] Molecular orbital energy.

[d] The organic ligand contributes the remainder to 100%.

greater than any dπ orbital in the *cis* isomer. The carboxyl function contributes 14–32% to the low lying π* orbitals in the *trans* isomer and in the *cis* isomer.

According to the ZINDO/S calculations there are three major absorption bands in these complexes in the visible and near UV region. The intense visible region absorption at 16 900 cm^{-1} is assigned to dπ(Ru) → π*(L) transition, i.e. HOMO (a) → LUMO (b) (with two other contributions, see Table 4) for the *cis* isomer, and HOMO (b$_3$) → LUMO (b$_1$) for the *trans* isomer. For the latter complex there is also an additional transition at 690 nm, which can also be assigned to an MLCT transition, HOMO-1 (b$_2$) → LUMO (b$_1$).

There are low intensity Ru d → d transitions in the visible region at 24 800 cm^{-1} for the *cis* isomer and 20 050 cm^{-1} for the *trans* isomer.

The intense UV region band near 320 nm is the internal π → π* ligand transition, formally, according to ZINDO/S calculations, from HOMO-4 and HOMO-5 (*cis* complex) to LUMO. The electronic spectra calculations are summarized in Table 4. Overall, there is excellent agreement between the experimental and predicted electronic spectra.

Table 4
Comparison between experimental and calculated (ZINDO/S) electronic[a,b]

Experiment	Calculated		
hν (cm^{-1})	*hν* (cm^{-1})	f	Assignment
cis-Ru(dcbpyH$_2$)$_2$Cl$_2$ (C_2 point group)			
16 950	17 100	0.377	101 → 102 (35%), 99 → 102 (28%), 100 → 103 (24%)
23 050	22 550	0.150	101 → 105 (56%)
	23 000	0.108	101 → 105 (55%), 101 → 104 (28%)
	23 450	0.353	100 → 104 (79%)
	23 900	0.104	99 → 105 (74%)
	24 800	0.031	101 → 114 (64%)
31 645	31 750	0.365	98 → 102 (34%), 97 → 103 (22%)
	31 950	0.198	100 → 115 (52%)
	32 500	0.951	97 → 102 (22%)
trans-Ru(dcbpyH$_2$)$_2$Cl$_2$ (D_2 point group)			
14 500	14 750	0.017	100 → 102 (94%)
16 900	17 250	0.431	101 → 102 (89%)
19 600	20 050	0.011	101 → 108 (89%)
22 700	23 250	0.374	100 → 103 (88%)
	23 900	0.256	101 → 103 (89%)
	25 200	0.106	99 → 105 (92%)
31 250	32 500	1.354	98 → 102 (38%)

[a] Spectra of Ru(dcbpyH$_2$)$_2$Cl$_2$.

[b] HOMO, 101; LUMO, 102; L, dcbpyH$_2$.

5. Conclusions

The electronic spectral properties of *cis*- and *trans*-[Ru(dcbpyH$_2$)$_2$(X)$_2$] (where X = Cl$^-$, H$_2$O, NCS$^-$) complexes were examined. The absorption and emission maxima of the MLCT bands in the spectra of the *trans* complexes are red shifted compared with its *cis* analogues. There is excellent agreement between the experimental and predicted spectra of both the *cis* and *trans* complexes. The ^{13}C-NMR data unambiguously show that the complexes containing thiocyanate ligands are N-coordinated. The discovery that *trans* complexes exhibit enhanced light harvesting in the red and near IR region opens up the way to improve significantly the overall efficiency of nanocrystalline photovoltaic devices. On the other hand, to improve the synthetic yields of the *trans* isomers one has to engineer at a molecular level using novel ligands.

Further details on the molecular orbital energies and mixing in the *cis*- and *trans*-dichloro species can be found at: http://www.chem.yorku.ca/profs/lever following the publications link to this paper.

Acknowledgements

Acknowledgements are made to the Swiss Energy Office (OFEN) and the Institut für Angewandte Photovoltaik (INAP), Germany, for support of this work. S.I.G. and A.B.P.L. thank the Natural Sciences and Engineering Research Council (Ottawa) for financial support.

References

[1] (a) T.J. Meyer, Pure Appl. Chem. 50 (1986) 1293. (b) D.M. Roundhill, Photochemistry and Photophysics of Metal Complexes, Plenum Press, New York, 1994.

[2] (a) K. Kalyanasundaram, M. Grätzel, Photosensitization and Photocatalysis using Inorganic and Organometallic Compounds, Kluwer, Dordrecht, 1993. (b) A. Juris, V. Balzani, F. Barigelletti, S. Campagna, P. Belser, A. von Zelewsky, Coord. Chem. Rev. 84 (1988) 85.

[3] (a) F. Scandola, C.A. Bignozzi, M.T. Inddelli, Photosensitization and Photocatalysis Using Inorganic and Organometallic Compounds, Kluwer, Dordrecht, The Netherlands, 1993, pp. 161–216. (b) M. Alebbi, C.A. Bignozzi, T.A. Heimer, G.M. Hasselmann, G.J. Meyer, J. Phys. Chem. B 102 (1998) 7577.

[4] Md. K. Nazeeruddin, A. Kay, I. Rodicio, R. Humphry-Baker, E. Müller, N. Vlachopoulos, M. Grätzel, J. Am. Chem. Soc. 115 (1993) 6382.

[5] (a) R.A. Krause, Inorg. Chim. Acta 22 (1977) 209. (b) B. Durham, S.R. Wilson, D.J. Hodges, T.J. Meyer, J. Am. Chem. Soc. 102 (1980) 600. (c) J.L. Walsh, B. Durham, Inorg. Chem. 21 (1981) 329. (d) P. Bonneson, J.L. Walsh, W.T. Pennington, A.W. Cordes, B. Durham, Inorg. Chem. 22 (1983) 1761. (e) B.J. Coe, T.J. Meyer, Inorg. Chem. 32 (1993) 4012. (f) M.A. Masood, B.P. Sullivan, D.J. Hodges, Inorg. Chem. 33 (1994) 5360. (g) B.J. Coe, T.J. Meyer, P.S. White, Inorg. Chem. 34 (1995) 593. (h) N.R. Weathers, R.C. Sadoski, B. Durham, A.W. Cordes, Acta Crystallogr. 53 (1997) 1047.

[6] D. Hesek, Y. Inoue, R.L. Everitt, Chem. Lett. (1999) 109.

[7] (a) J.B. Asbury, R.J. Ellingson, H.N. Ghosh, S. Ferrere, A.J. Nozik, T. Lian, J. Phys. Chem. B 103 (1999) 3110. (b) A. Zaban, S. Ferrrere, J. Sprague, B.A. Gregg, J. Phys. Chem. B 101 (1997) 55.

[8] (a) A.M. Bond, G.B. Deacon, J. Howitt, D.R. MacFarlane, L. Spiccia, G. Wolfbauer, J. Electrochem. Soc. 146 (1999) 648. (b) T. Hannappel, B. Burfeindt, W. Storck, F. Willig, J. Phys. Chem. B 101 (1997) 6799.

[9] (a) L. Dloczik, O. Ileperuma, I. Lauermann, L.M. Peter, E.A. Ponomarev, G. Redmond, N.J. Shaw, I. Uhlendorf, J. Phys. Chem. B 101 (1997) 10281. (b) J.S. Salafsky, W.H. Lubberhuizen, E. van Faassen, R.E.I. Schropp, J. Phys. Chem. B 102 (1998) 766.

[10] (a) H. Sughihara, L.P. Singh, K. Sayama, H. Arakawa, Md. K. Nazeeruddin, M. Grätzel, Chem. Lett. (1998) 1005. (b) K. Murakoshi, G. Kano, Y. Wada, S. Yanagida, H. Miyazaki, M. Matsumoto, S. Murasawa, J. Electroanal. Chem. 396 (1995) 27.

[11] (a) M. Alebbi, C.A. Bignozzi, T.A. Heimer, G.M. Hasselmann, G.J. Meyer, J. Phys. Chem. B 102 (1998) 7577. (b) R. Argazzi, C.A. Bignozzi, G.M. Hasselmann, G.J. Meyer, Inorg. Chem. 37 (1998) 4533.

[12] (a) C. Nasr, S. Hotchandani, P.V. Kamat, J. Phys. Chem. B 102 (1998) 4944. (b) M. Ihara, K. Tanaka, K. Sakaki, I. Honma, K. Yamada, J. Phys. Chem. B 101 (1997) 5153.

[13] P. Liska, N. Vlachopoulos, Md. K. Nazeeruddin, P. Compte, M. Grätzel, J. Am. Chem. Soc. 110 (1988) 3686.

[14] (a) Md. K. Nazeeruddin, S.M. Zakeeruddin, R. Humphry-Baker, M. Jirousek, P. Liska, N. Vlachopoulos, V. Shklover, C.H. Fisher, M. Grätzel, Inorg. Chem. 38 (1999) 6298. (b) V. Shklover, Yu. E. Ovchinnikov, L.S. Braginsky, S.M. Zakeeruddin, A. Kay, M. Grätzel, Chem. Mater. 10 (1998) 2533. (c) Md. K. Nazeeruddin, S.M. Zakeeruddin, R. Humphry-Baker, M. Graetzel, Inorg. Chim. Acta 296 (1999) 250.

[15] M.J. Cook, A.P. Lewis, G.S.G. McAuliffe, Org. Magn. Reson. 22 (1984) 388.

[16] Md. K. Nazeeruddin, P. Péchy, M. Grätzel, Chem. Commun. (1997) 1705.

[17] M.J. Root, P.B. Sullivan, T.J. Mayer, E. Deutsch, Inorg. Chem. 24 (1985) 2731.

[18] A.B.P. Lever, Inorg. Chem. 29 (1990) 1271.

[19] P. Sutra, M. Pink, A. Juris, M. Venturi, V. Balzani, C. Mingazzini, S. Serroni, S. Campagna, 13th International symposium on photochemistry and photophysics of coordination compounds, Isle of Lipari, Italy, 1999, p. 84.

[20] Gaussian 98, Revision A.7, M.J. Frisch, G.W. Trucks, H.B. Schlegel, G.E. Scuseria, M.A. Robb, J.R. Cheeseman, V.G. Zakrzewski, J.A. Montgomery Jr., R.E. Stratmann, J.C. Burant, S. Dapprich, J.M. Millam, A.D. Daniels, K.N. Kudin, M.C. Strain, O. Farkas, J. Tomasi, V. Barone, M. Cossi, R. Cammi, B. Mennucci, C. Pomelli, C. Adamo, S. Clifford, J. Ochterski, G.A. Petersson, P.Y. Ayala, Q. Cui, K. Morokuma, D.K. Malick, A.D. Rabuck, K. Raghavachari, J.B. Foresman, J. Cioslowski, J.V. Ortiz, B.B. Stefanov, G. Liu, A. Liashenko, P. Piskorz, I. Komaromi, R. Gomperts, R.L. Martin, D.J. Fox, T. Keith, M.A. Al-Laham, C.Y. Peng, A. Nanayakkara, C. Gonzalez, M. Challacombe, P.M.W. Gill, B. Johnson, W. Chen, M.W. Wong, J.L. Andres, C. Gonzalez, M. Head-Gordon, E.S. Replogle, J.A. Pople, Gaussian, Inc., Pittsburgh PA, 1998.

[21] (a) HyperChem for Windows, Release 5.1 Professional Version, Hypercube, Inc., Gainesville, Florida, USA, 1997. (b) M.C. Zerner, ZINDO program, version 98.1, Quantum Theory Project, University of Florida, Gainesville, FL.

[22] A.D. Becke, J. Chem. Phys. 98 (1993) 5648.

[23] C. Lee, W. Yang, R.G. Parr, Phys. Rev. B 37 (1988) 785.

[24] (a) T.H. Dunning Jr., P.J. Hay, in: H.F. Schaefer III (Ed.), Modern Theoretical Chemistry, vol. 3, Plenum, New York, 1976, p. 1. (b) P.J. Hay, W.R. Wadt, J. Chem. Phys. 82 (1985) 270. (c) P.J. Hay, W.R. Wadt, J. Chem. Phys. 82 (1985) 284. (d) P.J. Hay, W.R. Wadt, J. Chem. Phys. 82 (1985) 299.

[25] K. Krogh-Jespersen, J.D. Westbrook, J.A. Potenza, H.J. Schugar, J. Am. Chem. Soc. 109 (1987) 7025.

[26] $I_s = 25.23$ eV, $I_p = 15.03$ eV, $\beta_s = \beta_p = -10.5$ eV, $\zeta_s = \zeta_p = 2.033$, $F^2(\mathrm{p,p}) = 5.21$ eV, $G^1(\mathrm{s,p}) = 2.66$ eV, $\gamma(\mathrm{ss}) = 11.41$ eV (taken from S.I. Gorelsky, V. Yu. Kotov, Russ. J. Coord. Chem. 24 (1998) 491.